Salient difference of sea surface temperature over the North Atlantic in the spring following three super El Niño events

Jinhua Yu, Xuyu Zhang, Laurent Li, Chunhua Shi, Yangbo Ye

Salient difference of sea surface temperature over the North Atlantic in the spring following three super El Niño events

Environmental Research Letters

LETTER

Salient difference of sea surface temperature over the North Atlantic in the spring following three super El Niño events

Jinhua Yu[1], Xuyu Zhang[1], Laurent Li[2], Chunhua Shi[1] and Yangbo Ye[1]

[1] Key Laboratory of Meteorological Disaster, Ministry of Education (KLME)/ Collaborative Innovation Center on Forecast and Evaluation of Meteorological Disasters (CIC-FEMD), Nanjing University of Information Science and Technology, Nanjing 210044, People's Republic of China

[2] Laboratoire de Météorologie Dynamique, CNRS, Sorbonne Université, Ecole Normale Supérieure, Ecole Polytechnique, Paris, France

E-mail: jhyu@nuist.edu.cn and jhyu64@163.com

Keywords: North Atlantic SSTA, super El Niño events, teleconnection

OPEN ACCESS

RECEIVED
23 March 2020

REVISED
18 June 2020

ACCEPTED FOR PUBLICATION
2 July 2020

PUBLISHED
21 August 2020

Abstract

Despite similar evolution of Niño3.4 index for three strong El Niño events in the tropical Pacific in 1982–1983, 1997–1998 and 2015–2016, divergent sea surface temperature anomalies (SSTAs) were observed in the North Atlantic (NA) in spring following El Niño peak. Strong teleconnection occurred for the first two events in 1982–1983 and 1997–1998, leading to a negative phase of a North Atlantic Oscillation-like circulation over the extratropical NA, and thus a positive tripolar SSTA pattern in the NA. But the teleconnection was weak for the case of 2015–2016 El Niño, the SSTA in spring 2016 in NA being mainly created and maintained by the preconditioning of the NA basin and local atmosphere-ocean interactions. The salient difference among the three events resides in their ways to operate the teleconnection linking the central-eastern equatorial Pacific and the subtropical eastern North Pacific to the extratropical NA, which would be a key to explain the different impacts of the three exceptional El Niño events. It is furthermore shown that the reduced anomalous westerlies over Central America along 30° N around the peak time of 2015–2016 El Niño play a role of inhibition for an efficient Rossby wave energy propagation from the tropics, eastward into the Gulf of Mexico and northward into midlatitudes in the western NA.

1. Introduction

The El Niño-Southern Oscillation (ENSO) is an important interannual variability component of the climate system. It typically develops during boreal spring and summer, peaks in winter in the equatorial central-eastern Pacific, and decays in the following spring and summer. ENSO is the result of complex ocean-atmosphere coupling in the tropical Pacific and presents strong irregularity for both its periodicity and amplitude. Accompanying ENSO, positive sea surface temperature anomalies (SSTAs) generally occur over the tropical North Atlantic (NA), with a tripolar structure for the whole North Atlantic basin. Such SST anomalies in NA can exert important impacts on the regional climate (Rodwell *et al* 1999, Czaja and Frankignoul 2002, Li and Conil 2003, Msadek *et al* 2011, Wang *et al* 2009). It is generally agreed that SST anomalies in NA are caused (at least partly) by ENSO through global atmospheric bridges. A few hypotheses can be found in literature to explain the linkage.

El Niño can firstly perturb the atmospheric circulation to weaken the northeasterly trade winds over the tropical NA (Hastenrath *et al* 1987), to reduce surface evaporation and ultimately warm the SST. The anomalous southwesterly winds over the tropical NA are linked to weakening of the Azores high, as a part of the El Niño-induced Pacific/North American pattern (PNA, Wallace and Gutzler 1981). They are also revealed to be related to the eastward shift of the Walker circulation, and the reduction of the Atlantic Hadley cell (Klein *et al* 1999, Wang *et al* 2005). All these changes are direct consequences of El Niño from the Tropical Pacific. It is also shown that a remote Gill-type response to El Niño, manifested as a heat source over the Amazon basin (García-Serrano *et al* 2017), can contribute significantly to the reduction of

trade winds over the tropical NA. Finally, a reduction of cloudiness associated with the descending branch of the anomalous Walker circulation and the eastward propagation of a warm Kelvin wave (Lintner and Chiang 2007) are also powerful mechanisms to cause warming of the tropical NA via enhanced incoming solar radiation on the ocean surface (Klein *et al* 1999, Lau and Nath 2001, García-Serrano *et al* 2017). It is worthy to note the teleconnection pathways from ENSO to the North Atlantic can be nonlinear and highly dependent on the intensity of El Niño events, as shown with a series of numerical simulations reported in (Jiménez-Esteve and Domeisen 2020). Besides these tropospheric pathways, a few studies also revealed stratospheric mechanisms linking North Atlantic anomalies to ENSO through the stratospheric polar vortex or the circumpolar westerly jet (Butler *et al* 2014, Kidston *et al* 2015, Hardiman *et al* 2019).

In parallel to the general mechanisms mentioned above, some authors payed more attention to the particularity of individual El Niño events. Studies of (Toniazzo and Scaife 2006) show that strong El Niño events may excite a secondary energy source over the tropical Atlantic, which propagates northward, and thus forms a high geopotential height to the west of Europe. (Scaife *et al* 2017) argued the winter of 1982–1983 was closely analogous to winter 2015/2016 in both the predictable driving factors and the forecast winter circulation over Europe. (Lee *et al* 2008) showed that only El Niño events persisting beyond spring can force a significant warm SSTA over the tropical NA region during the decaying phase. A recent study carried out by (Taschetto *et al* 2016) indicated that the spring warming of SST in the tropical NA following El Niño events is associated with and conditioned by El Niño intensity in the tropical Pacific and preconditioning of the tropical NA in the previous winter. Their studies implied that strong and long-duration El Niños, such as 1982/1983 and 1997/1998 events, are favorable for warm SSTA to occur later in the tropical NA. Actually, the warm tropical NA reflects a positive tripolar SSTA pattern over the NA, which is the leading Empirical Orthogonal Function mode of SSTAs in the NA basin at interannual timescale (Czaja and Marshall 2001, Han *et al* 2016).

The evolution of Niño3.4 index during 2015/2016 was similar to those in 1982/1983, 1997/1998 with Niño3.4 index peak reaching around 2.4 °C in winter (figure 1(a)), and all three events persisted into the following spring. However, the SSTA pattern over the NA was a vigorous negative tripolar mode in the spring of 2016, which differed from the robust positive one in the spring of 1983 and 1998 (figure 1(b)). So far it is unclear why the 2015/2016 event behaved so differently from the other two events, despite their similar amplitude of SST anomalies over the tropical Pacific. The objective of this study is to reveal such differences and to investigate relevant physical mechanisms. Section 2 describes the data that we used and our analysis methodology. In section 3.1, we compare the basic characteristics of spring NA SSTAs corresponding to the three El Niño events. We present results on thermodynamic factors related to SSTA change in section 3.2. Results on atmospheric teleconnection from the central-eastern equatorial Pacific to NA are described in sections 3.3 and 3.4. We will show evidence that the weak teleconnection through the extratropical pathway during the peak of 2015–2016 El Niño is a key factor to explain the unusual behavior of NA SST anomalies and corresponding physical mechanisms.

2. Data and methodology

The global monthly SST data are from the Met Office Hadley Centre with a horizontal resolution of 1° (Rayner *et al* 2003). The Niño 3.4 index is the averaged SSTA over the region of 5° S–5° N, 170°–120° W. An anomaly of a variable is defined as a departure from its climatology averaged in the period of 1981–2010. The North Atlantic tripolar index (NA index), similar to that of (Czaja and Marshall 2001), refers to the average of the SSTAs in the tropical region (10°–20° N, 50°–20° W) and the middle-high latitude region (40°–55° N, 60°–30° W) minus the SSTA in the subtropical region (25°–35° N, 80°–50° W).

Monthly-mean atmospheric variables, with a latitude-longitude grid of 0.25 degrees, are from the reanalysis ERA5 provided by the European Center for Medium-Range Weather Forecasts (ECMWF). We also use the wave flux for a snapshot analysis of stationary or migratory eddies on a zonally varying basic flow (Takaya and Nakamura 2001) and the necessary daily data are from ERA5.

3. Results

3.1. Characteristics of spring NA SSTAs

Let us take a closer look at how El Niños and NA SSTA evolved for the 1982–1983, 1997–1998 and 2015–2016 El Niño events (figure 1). All the three events were observed to develop since spring and peak in winter when their Niño3.4 index reached about 2.4 °C. Gradually decreasing thereafter, they eventually turned to negative by June. Although their evolution was close to each other in the Tropical Pacific, variation of the NA index was different among the three El Niño events (figure 1(b)). During the 1982–1983 event, the NA index was negative in the El Niño developing and peak phases, and became robustly positive after the El Niño peak, with the SSTA index maximizing in April (1.1 °C). The positive state remained through to the following July. For the 1997–1998 event, the NA index oscillated between positive and negative during the developing phase and became robustly positive after the El Niño peak, with

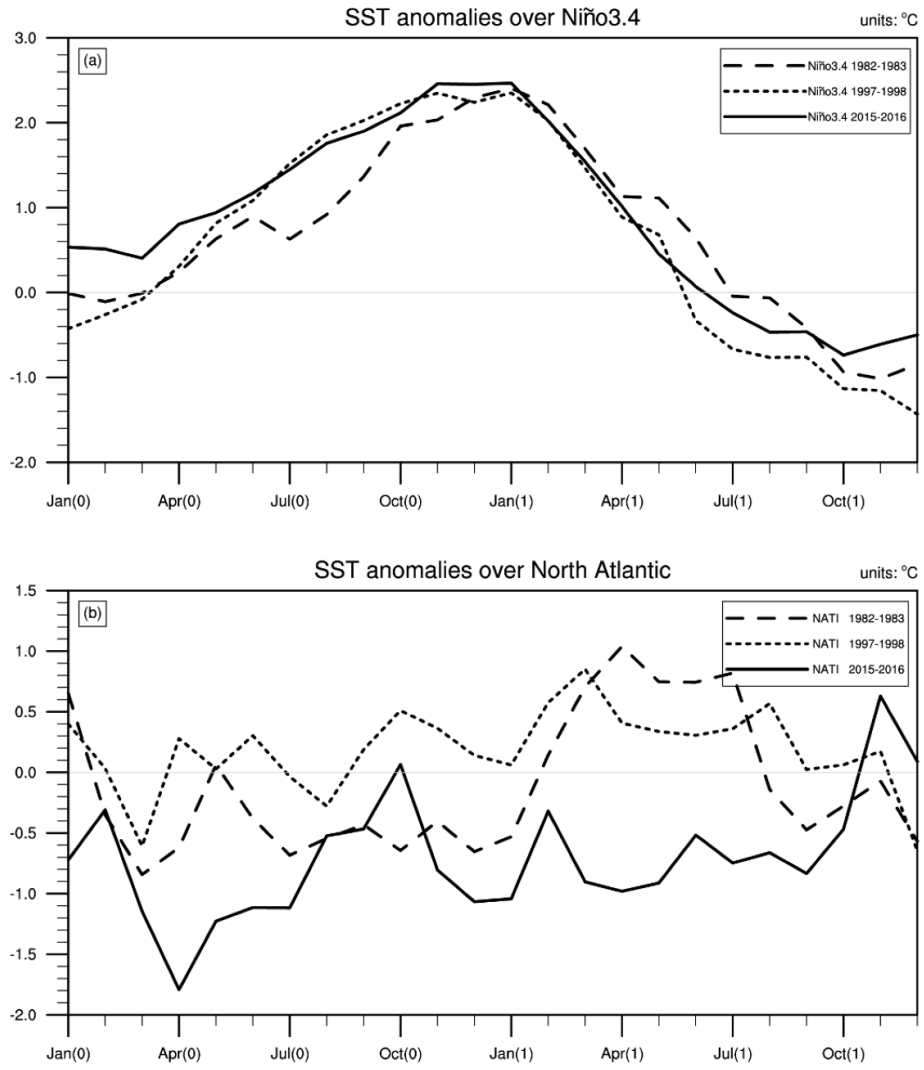

Figure 1. (a) Niño 3.4 index showing the areal-mean SST (°C) in the domain (5° S–5° N, 170°–120° W). (b) North Atlantic SSTA index (°C) with the average of the SSTAs in the tropical region (10°–20° N, 50°–20° W) and the middle-high latitude region (40°–55° N, 60°–30° W) minus the SSTA in the subtropical region (25°–35° N, 80°–50° W) . The three curves correspond to three strong El Niño events for 1982–1983 (dashed line), 1997–1998 (dotted line) and 2015–2016 (solid line). *X*-axis is the time in month, and numbers in parentheses denote years relative to the El Niño peak: 0 represents the developing year and 1 represents the decaying year.

the SSTA index maximizing in March (0.8 °C). The positive state remained elevated through the following August. The NA index was remarkably negative during the 2015–2016 El Niño's developing phase, and maintained negative during the spring and summer following the peak. Clearly, the NA SSTA pattern during the decaying phase of the 2015–2016 El Niño event was remarkably different from those for the 1997–1998 and 1982–1983 events.

Consistent with the NA index, spatial patterns of SSTA in NA show also significant differences among the three events, as shown in figure 2 (SSTA in spring at upper panels, SSTA variation from winter to spring at lower panels). Although positive SSTAs occurred over the tropical NA in March–May (spring) during the decaying phase for the three El Niño events (figures 2(a)–(c)), the warming was particularly pronounced for the spring of 1983 and 1998 (figures 2(a) and (b)) and almost nonexistent for the spring of 2016 (figure 2(c)). The other two poles of SSTA at mid and high latitudes show also opposite anomalies between 1982–1983 and 1997–1998 on the one hand and 2015–2016 on the other. Consequently, the SSTA structure in the NA resembled a positive tripolar mode during the decaying phase of the 1982–1983 and 1997–1998 El Niños (figures 2(a) and (b)), and a negative one for the 2015–2016 El Niño figure 2(c)).

Compared to the SSTA snapshot in spring, the evolution (or seasonal variation) of SSTA from the El Niño peak winter to the following spring (shown at the lower panels in figure 2) is more revealing for the underlying mechanisms linking El Niño in the Pacific to the tripolar SSTA in the North Atlantic. We found that the SSTA seasonal variation was the most robust during the 1982–1983 El Niño event. With significant positive values over the tropical and mid-high latitude NA and negative ones over the subtropical

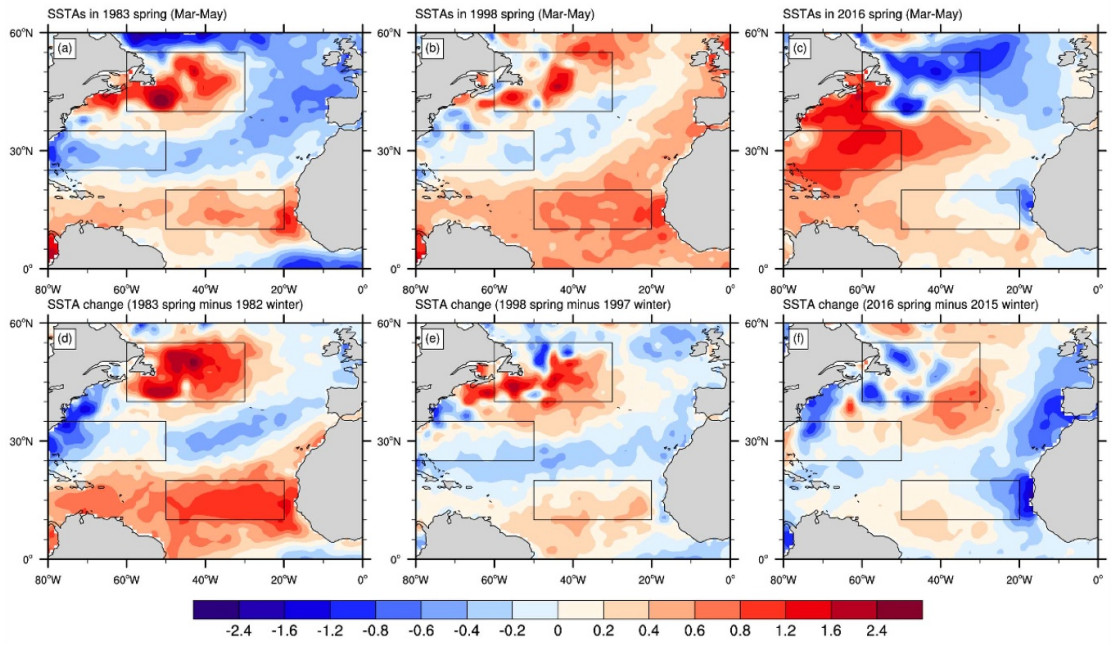

Figure 2. Spatial distribution of SSTAs (°C) over the North Atlantic (0°–80° W,0°–60° N) during boreal spring ((a)–(c)) and its seasonal variation from boreal winter to spring (d)–(f) for the 1982–1983 ((a), (d), left), 1997–1998 ((b), (e), middle) and 2015–2016 ((c), (f), right) El Niño events.

NA (figure 2(d)), it also had a typical positive tripolar pattern. The SSTA change pattern over the NA in the spring of 1998 (figure 2(e)) was similar to that of 1983, yet the amplitude was smaller. A remarkably different situation occurred for 2016, with very weak SSTA warming over the central tropical NA and cold SSTAs appeared over the east NA and western mid-high latitudes (figure 2(f)).

3.2. Thermodynamic processes associated with spring SSTA

In figure 3(a), we can see that significant anomalous negative (positive) latent heat fluxes appeared in February–April 1983 over the tropical and mid-high latitude (subtropical) NA. This means that the sea surface evaporation significantly decreased (increased), contributing to the robust positive (negative) SSTA variation in spring 1983 as shown in figure 2(d). The anomalous latent heat flux pattern over the NA in 1998 (figure 3(b)) was similar to that in 1983 except that its anomalous negative values over the tropical NA were weaker. In 2016, despite the fact that anomalous positive fluxes occurred at the eastern fringe of NA, the amplitude of anomalous negative latent heat fluxes over the major part of the tropical NA (figure 3(c)) was larger than that in 1998. The evaporation significantly increased (decreased) over mid-latitudes of the western NA in 2016 (1998), thus contributing to the negative (positive) SSTA change there in 2016 (1998) (figures 2(f) and (e)).

The net shortwave radiation flux increased over the central tropical NA following the peak of the three El Niño events. This increase was largest during 1998, and weakest in 2016 (figures 3(d)–(f)). Positive SSTA change over the central tropical NA was caused by both the latent heat flux decrease and the shortwave radiation increase in spring 1998, while it was merely associated with the former in spring 1983. During February–April 2016 (figure 3(f)), robust anomalous negative shortwave radiation occurred in the east NA, resulting in negative SSTA change (figure 2(f)) along with evaporation increase (figure 3(c)). Over the central tropical NA, the positive SSTA change was weaker in 2016 (figure 2(f)) than in 1998 (figure 2(e)), which is associated with weaker positive anomalous shortwave radiation flux in 2016 (shown in figures 3(f) and 3(e)) and interaction between atmosphere-ocean.

The evaporation variation is affected by both wind speed and vertical gradient of specific humidity between the surface and near-surface atmosphere. The anomalous latent heat flux can be thus decomposed into two parts, associated with wind speed (figure 3, third row) and water vapor gradient (figure 3, last row), respectively. Figures 3(g) and (j) show that the decreased evaporation over the tropical NA in figure 3(a) is largely attributable to the reduction of wind speed during February–April 1983. An anomalous cyclonic circulation occurred in the subtropical NA, producing tropical anomalous southerlies and westerlies, and thus reducing the wind speed (figure 3(g)). Due to a weaker subtropical anomalous cyclonic circulation, the evaporation

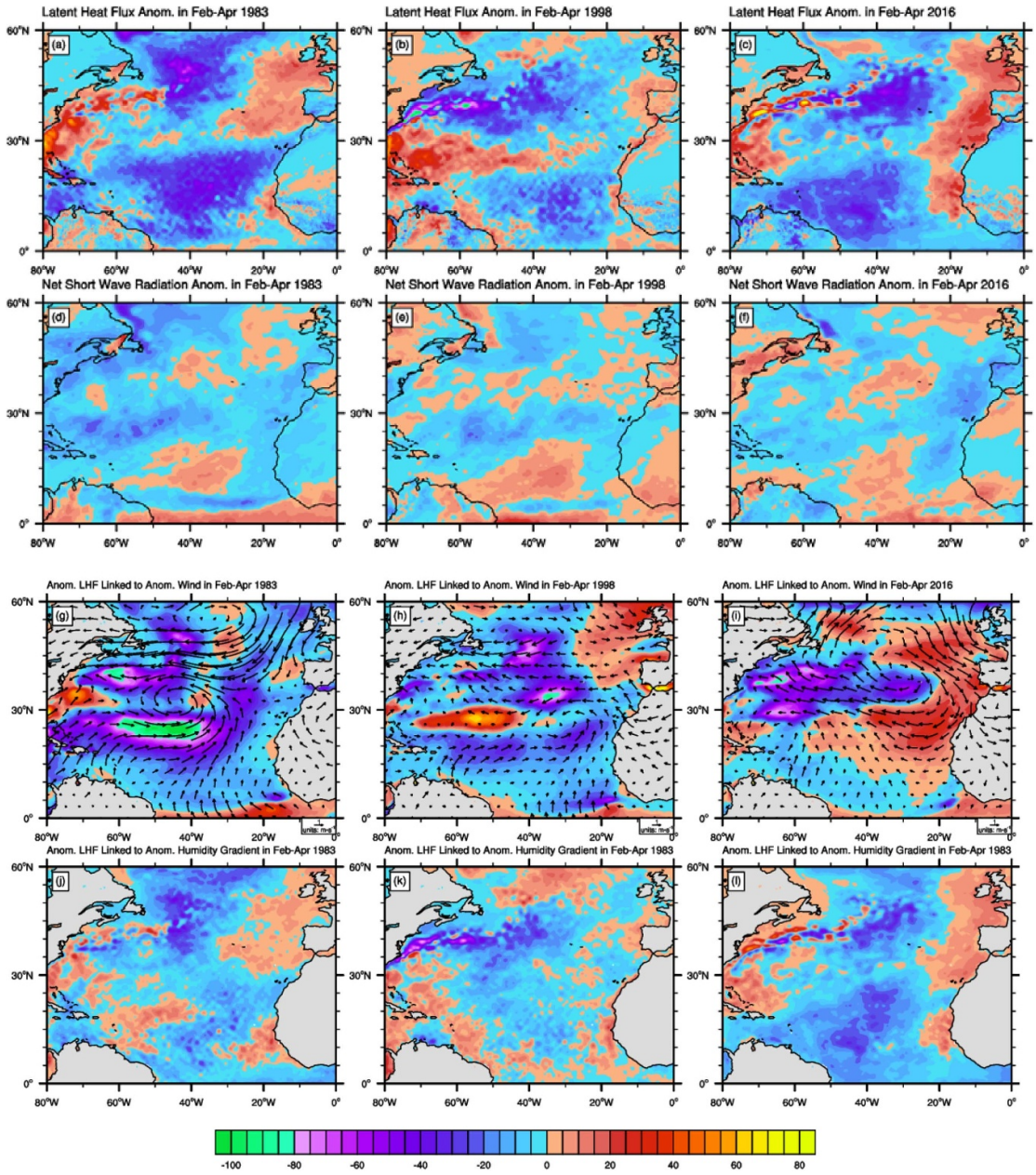

Figure 3. Anomalous February–April latent heat flux ((a)–(c), up is positive and down is negative) and net short-wave radiation ((d)–(f)), up is negative and down is positive), February–April anomalous wind vector (units: $m \cdot s^{-1}$) at surface and anomalous latent heat flux associated with wind speed anomalies (shading, (g)–(i)) and vertical humidity gradient anomalies between sea surface and 2 m height ((j)–(l)) for 1983 ((a), (d), (g), (j)), 1998 ((b), (e), (h), (k)) and 2016 ((c), (f), (i), (l)). The units of latent heat flux and net short-wave radiation is $W \cdot m^{-2}$.

variation associated with the anomalous wind speed over the tropical NA during February–April 1998 (figure 3(h)) was smaller than that in 1983, leading to a smaller anomalous negative latent heat flux as shown in figure 3(b). During February–April 2016, the evaporation reduction over the central tropical NA (figure 3(c)) was mainly related to increase of humidity vertical gradient (figure 3(l)), reflecting that the SSTA change there in spring 2016 was mainly associated with regional processes of atmosphere-ocean interaction, not remote atmospheric forcing as in spring 1983 and 1998.

3.3. Atmospheric bridges from the tropical Pacific to NA

The shading in figure 4 displays the geopotential height (GH) anomalies at 500 hPa. A tripolar structure of high-low-high along a great-circle path shows a typical Pacific-North American (PNA) teleconnection pattern (Wallace and Gutzler 1981), while the position and amplitude of the PNA pattern's anomalous center were different among the three El Niño events. During January–March 1983 (figure 4(a)), the most robust negative GH anomalies, as usual, occurred over the central-eastern North Pacific, while

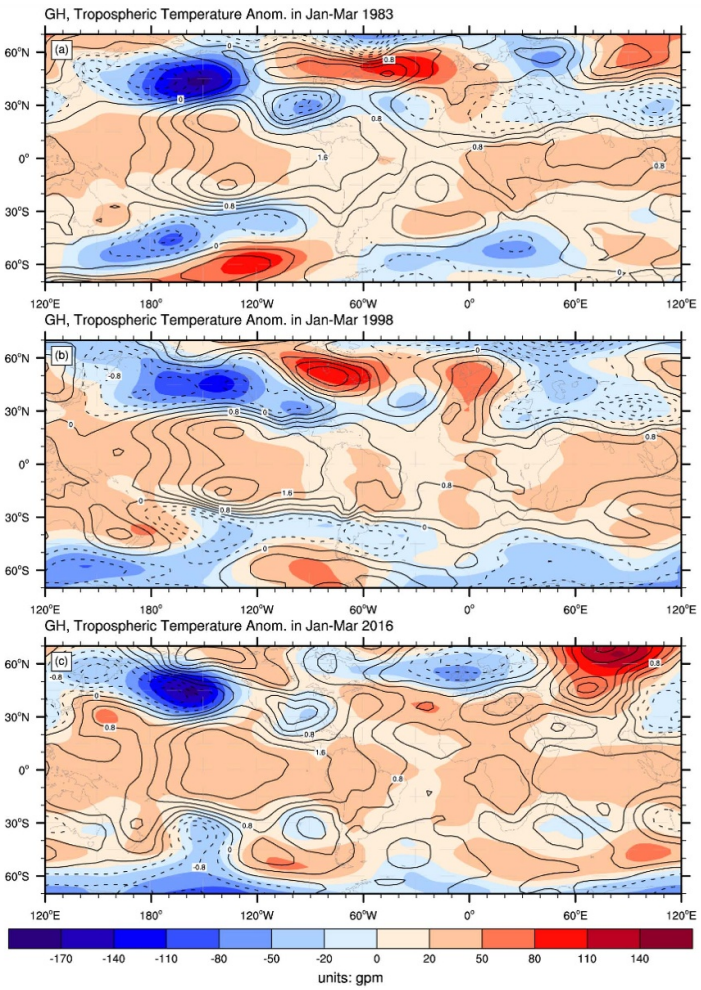

Figure 4. Anomalous January–March geopotential height (shading, units: gpm) at 500 hPa and tropospheric temperature from 1000 to 200 hPa (contour, solid lines represent positive anomalies and dashed ones do negative anomalies, units: °C) for 1983 (a), 1998 (b) and 2016 (c).

robust positive ones extended from North America to the NA (figure 4(a)). An obvious chain of cores of negative height anomalies in the mid-latitude Northern Hemisphere resembled a zonally damped wavy structure with wave number 5 along 30° N, which looks like a circum-global teleconnection pattern. The subtropical centers of negative anomalies were situated over the eastern North Pacific, the southern United States, the subtropical NA, central Europe to the Middle East, and finally, northern India and central China. Over the Atlantic, the dipolar anomaly at extratropical latitudes was reminiscent of a negative North Atlantic oscillation (NAO)-like (Czaja and Marshall 2001) atmospheric circulation and a response to strong El Niño forcing (Jiménez-Esteve and Domeisen 2020). This height anomaly and its associated anomalous cyclonic circulation (figure 3(g)) tended to weaken the subtropical high system, reducing the surface northeast trade winds in the tropical region in the winter to spring period (figure 3(g)), and diminishing the evaporative cooling at the surface during the spring (figure 3(a)).

During January–March 1998 (figure 4(b)), a large negative center of PNA was located to the east of 150° W with an amplitude weaker than that of 1983 (figures 4(b) VS 4(a)). Large positive geopotential height anomalies mainly occurred over North America and did not stretch into the NA, leading to weaker positive height anomalies in the high-latitude NA. A zonally damped wavy structure with wave number 4 or 5 is close to that in 1983, and appeared in the subtropics, causing a weaker negative NAO-like atmospheric circulation over the extratropical NA. As shown in figure 3(h), this resulted in an anomalous anticyclonic circulation in the high latitudes and a cyclonic one in the subtropical NA.

For the 2015–2016 El Niño case, the positive GH anomaly over the tropics was the most pronounced, and the amplitude of negative anomalies centered over the central-eastern North Pacific matched that of 1983 (figures 4(c) VS 4(a)). However, the amplitude of positive anomalies over North America was the weakest among the three El Niño events. Anomalous positive GH occurring in the west of

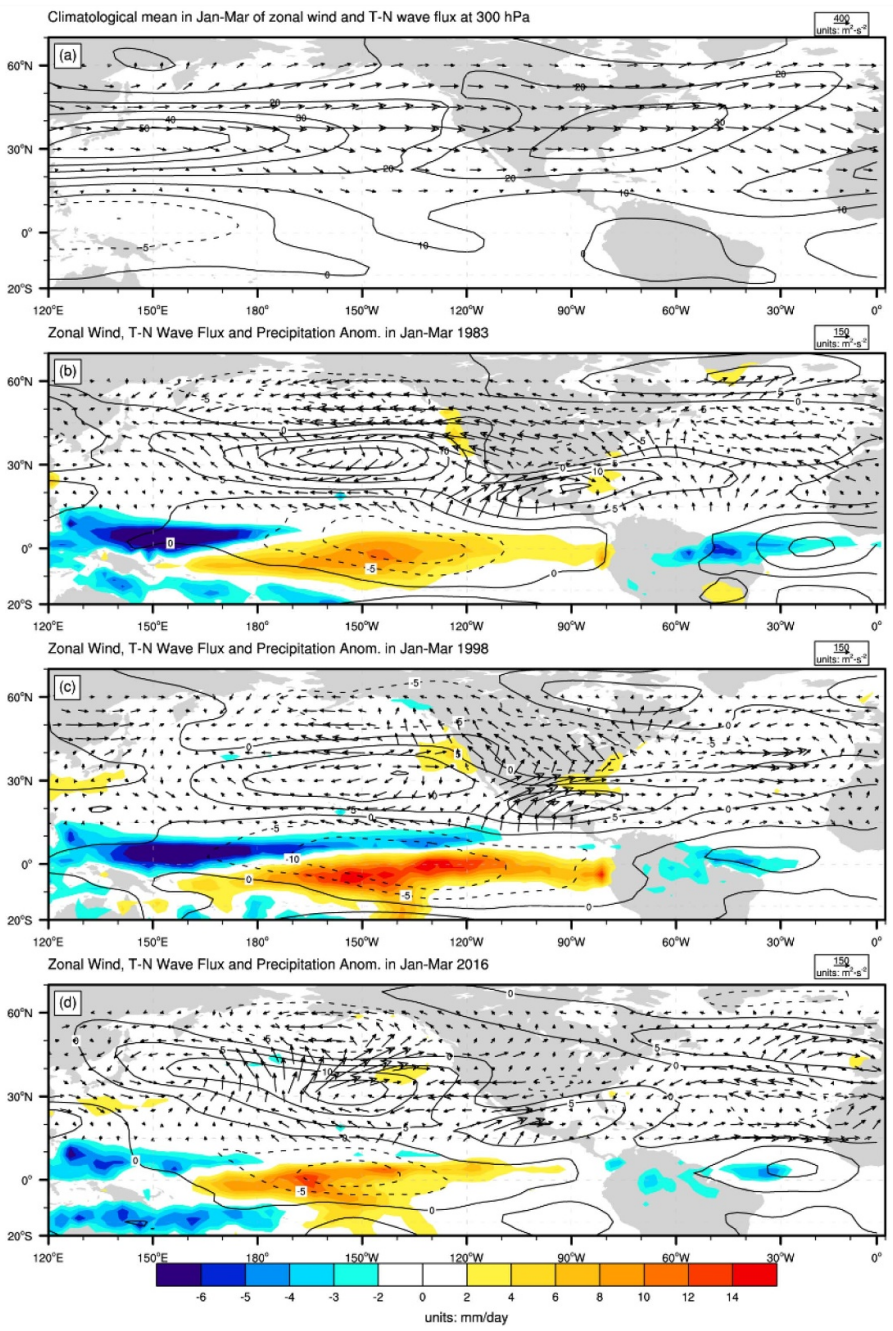

Figure 5. (a) Climatological January–March mean wave activity flux (vector) and zonal wind (contour, units: $m \cdot s^{-1}$) at 300 hPa. Anomalous January–March zonal wind (contour, solid lines represent zonal westerlies and dashed ones show zonal easterlies, units: $m \cdot s^{-1}$) and wave activity flux (vector) at 300 hPa for 1983 (b), 1998 (c) and 2016 (d) from the mean in (a). The shading means anomalous precipitation (units: mm d^{-1}) during January–March 1983 (b), 1998 (c) and 2016 (d).

America did not stretch into the NA, leading to a negative GH anomaly there in 2016 (figure 4(c)). The negative GH anomaly propagating into the southern United States was much weaker than that of 1983 and 1998 and did not stretch into the subtropical NA. A significant positive GH anomaly occurred over the mid-latitude NA (figure 4(c)). Different from that shown in some of the previous studies (Graf and Zanchettin 2012, Zhang *et al* 2019), we found that the dipolar GH anomaly over the extratropical NA manifested a positive NAO-like atmospheric circulation, which is thought to be remotely associated with the warm eastern basin of the subtropical North Pacific. The very active tropical-cyclone season in the Central Pacific in 2015 boreal summer was demonstrated (Murakami *et al* 2017) to be the consequence of warm subtropical SST, not very much in relation to the El Niño emblematic warming over the tropical Pacific. We examined one of the sensitivity experiments conducted in (Murakami *et al* 2017) with actually-observed warming SST over the subtropical eastern Pacific (10°–35° N, 150°–100° W) prescribed in GFDL (Geophysical Fluid Dynamics Laboratory) atmospheric model (AM2.5), and we

obtained (not shown) a spatial 500 hPa geopotential structure that looks like the NAO positive phase over the extratropical NA and positive GH anomalies over the East Pacific, off the American coast. The simulation largely reproduced the observed positive GH anomaly off the Californian coast and extended into midlatitudes (figure 4(c)). However, the negative NAO-like circulation during the peak of 1982–1983 and 1997–1998 was caused by the central-eastern equatorial El Niño teleconnection forcing.

Contours in figure 4 display the anomalous tropospheric temperature for the three El Niño events. In a large tropical belt, we can clearly see the eastward propagation of warm equatorial Kelvin waves excited from the eastern equatorial Pacific, which induces a general warming of the troposphere. A warmer troposphere can increase its static stability, and thus enhances the net solar radiation (figures 3(d)–(f)) with less clouds. The propagation of warm Kelvin waves in 2016 was similar to that in 1998, with the anomalous temperature reaching 0.8 °C over the tropical Atlantic, which reduces the latent heat flux, as shown in figure 3(l), due to decreased vertical gradient of temperature. We can now attempt to conclude that, among the three El Niño events, atmospheric bridges through tropical circulations (including zonal and meridional overturning cells, equatorial warm Kelvin waves) were similar to each other. So, for those exceptional El Niño events, different propagations of Rossby waves over the extratropical regions are the key to understand the salient SSTA changes over the NA.

3.4. Wave activity fluxes dissipating tropical Pacific perturbations to NA

We now examine the 300 hPa zonal winds and wave activity fluxes (Takaya and Nakamura 2001) displayed in figure 5(a) for long-term climatology and in figures 5(b)–(d) for anomalous fields corresponding to the three El Niño events, respectively. Besides the obvious jet stream cores over the North Pacific and North Atlantic, we can also observe westerly winds over the central-eastern equatorial Pacific, a favorable window for tropical perturbations to propagate to extratropical regions (Wen *et al* 2019). In figure 5(b) displaying anomalous fields for January–March 1983, we can see that anomalous westerlies occur over the subtropical North Pacific (the exit region of the East Asian jet stream) and over Central America with extension to the NA. These two regions constitute the key pathways for Rossby waves to dissipate energy of latent heat release from the tropics to extra-tropics, as revealed by the T-N wave activity fluxes. What shown here is consistent with the well-established theoretical considerations as described in (Webster 1981, 1982, (Hoskins and Karoly 1981), among many others. The northward propagating pathway is tightly related to the PNA pattern (figure 4(a)) with downstream extension to the NA. The northeastward pathway through Central America allows energy to propagate from the tropics to the subtropical North Atlantic, and furthermore to propagate through the subtropical jet playing the role of a wave guide (Hoskins and Ambrizzi 1993, Graf and Zanchettin 2012). Simultaneously, a Rossby wave train also emanates from the tropical North Atlantic and propagates northward to higher latitudes, contributing certainly to the negative NAO-like circulation as shown in figure 4(a). The northward propagation branch is consistent with the WKB (Wentzel-Kramers-Brillouin approximation) ray-path for stationary Rossby waves emanating from deep tropical Atlantic (Toniazzo and Scaife 2006).

During January–March 1998 (figure 5(c)), although the anomalous precipitation over the equatorial Pacific exceeded that of 1983, the anomalous westerlies over the subtropical North Pacific and over Central America are weaker than those in 1983. Consequently, the Rossby wave energy propagation from the tropics to midlatitudes during 1998 was weaker, leading to a center of weaker negative GH anomalies over the eastern North Pacific at upper troposphere and weaker negative NAO-like circulation (figures 4(b) VS 4(a)).

In figure 5(d) showing anomalous fields during January–March 2016, we can see enhanced precipitation over the equatorial Pacific between 180° and 150° W, with an anomalous center overpassing that of 1983 while westward shifted. The anomalous westerlies over the subtropical North Pacific are weaker than those in 1983, mainly due to low-frequency interdecadal variability. This may be associated with warm SSTs in the subtropical eastern North Pacific (Murakami *et al* 2017) and in the western subtropical NA (figure 2(c)). With decreased meridional temperature gradient, weaker westerlies are observed over the subtropical North Pacific and NA for the 2015–2016 El Niño event. Such a situation is favorable for Rossby waves to dissipate energy preferentially through the west pathway over the North Pacific, making negative geopotential height anomalies over the eastern North Pacific, as shown in figure 4(c). Weaker anomalies of zonal wind along 30° N over Central America are not favorable for waves to propagate into the Gulf of Mexico. In addition, the smaller anomalies of zonal wind over the subtropical western North Atlantic hinder the northward propagation of Rossby waves emanated from the tropical Atlantic. Instead, eastward wave propagation is found over the tropical North Atlantic (figure 5(d)). The positive NAO phase that we observed in spring 2016 is certainly a manifestation that it resulted from warm subtropical eastern North Pacific and local coupling between ocean and atmosphere over

the NA. The atmospheric response over the Atlantic to the heat forcing over the central-eastern equatorial Pacific during 2016 was much weaker than that during 1983 and 1998.

4. Conclusion and discussion

This paper focused on spring SSTA (sea-surface temperature anomaly) in the NA (North Atlantic) basin following three super El Niño events in 1982–1983, 1997–1998 and 2015–2016. The three exceptional events in the tropical Pacific showed a similar evolution for their Niño3.4 index, but SSTA in the NA presented salient differences in both spatial structure and temporal evolution. We investigated the NA SSTA spatial distributions, factors affecting SSTA seasonal evolution and associated anomalous atmospheric circulation. Besides the potential influences from the stratospheric polar vortex (actually, the stratospheric wind is strengthened in 2015–2016 winter) and the preconditioning of the NA itself, our main effort was on physical mechanisms operating in the troposphere to lead to different atmospheric responses of the NA to adiabatic heating over the equatorial Pacific.

For the 2015–2016 event, the NA SSTA merely changed from the El Niño peak to the following spring, which was very different from the cases of 1982–1983 and 1997–1998. Actually, significant positive SSTA variation from winter to spring was observed over the tropical and high-latitude NA for the 1982–1983 El Niño event, while robust cooling occurred over the eastern NA in spring 2016.

Our work confirms the conclusion of previous studies and shows that warm SST anomalies occurring in the tropical NA were generally associated with a decrease of evaporation at the sea surface. The reduction of evaporative cooling over the tropical NA essentially resulted from attenuated trade wind during early spring in 1983 and 1998. But this anomalous warming was essentially related to a smaller temperature gradient between the sea surface and the surface air in early spring 2016. We can conclude that the SSTA variation from winter to spring in 1983 and 1998 was mainly connected to remote atmospheric forcing, but it was largely determined by local interaction between atmosphere and ocean in 2016.

A typical high-low-high PNA pattern occurred during late winter for all the three El Niño events. However, positive (negative) geopotential height anomalies existed in the high latitude (subtropical) NA in January–March 1983, leading to a negative NAO-like circulation. In comparison, the anomalous positive GH over the NA in January–March 1998 was weaker, leading to a weaker anomalous cyclonic circulation over the subtropical NA. In the contrary, in January–March 2016, an anomalous anticyclonic circulation occurred over the mid-latitude NA, which was associated with the positive NAO-like circulation. The salient difference of atmospheric circulation over the extratropical NA for the three different El Niño events appears to be a consequence of different ways of teleconnection from the equatorial Pacific to the NA. Our results suggest that the response of atmospheric circulation at upper troposphere over the extratropical NA depends on not only the intensity and position of anomalous latent heat release over the equatorial Pacific but also the seasonal-mean zonal wind structure over the equatorial Pacific and the extratropical North Pacific and Atlantic. The faint teleconnection from the equatorial Pacific to the extratropical NA for the 2015–2016 El Niño event is believed to be associated with smaller precipitation anomalies over the eastern equatorial Pacific and with weakened zonal westerlies along 30° N, which suppressed the Rossby wave energy's meridional propagation from the eastern tropical Pacific to subtropical latitudes and from tropical Atlantic to midlatitudes. As a result, only weak anomalous negative GH was induced to Central America and a weak positive NAO-like circulation over the extratropical NA.

Our results also confirmed the important role of warm SST anomalies that occurred in the eastern basin of the subtropical North Pacific and the western basin of the subtropical NA in 2015–2016. They decreased the meridional temperature gradient of the two basins, and thus produced weaker westerly anomalies over the subtropical North Pacific and NA. Actually, such a situation of weak zonal wind anomalies is not favorable to have a strong teleconnection forcing from the tropical Pacific to North Atlantic. It is also worthy to note that the significant warm SST in the subtropical eastern North Pacific during the 2015–2016 El Niño event has a strong interdecadal signal.

Acknowledgments

We thank two anonymous reviewers and Professor Wenju Cai for their constructive and helpful comments on an earlier manuscript and Dr Murakami for providing us his model results. This work was supported by the National Key R&D Program of China (2018YFC1507704) and the National Natural Science Foundation of China Grant (41575083, 41730961). The SST data were retrieved from https://climatedataguide.ucar.edu/climate-data/sst-data-hadisst-v11. The reanalysis data for monthly-mean and daily atmospheric variables and surface latent heat flux were from www.ecmwf.int/en/forecasts/datasets/reanalysis-datasets/era5.

References

Butler A H, Polvani L M and Deser C 2014 Separating the stratospheric and tropospheric pathways of El Niño–Southern Oscillation teleconnections *Environ. Res. Lett.* **9** 024014

Czaja A and Frankignoul C 2002 Observed impact of Atlantic SST anomalies on the North Atlantic Oscillation *J. Clim.* **15** 606–23

Czaja A and Marshall J 2001 Observations of atmosphere-ocean coupling in the North Atlantic *Q. J. R. Meteorol. Soc.* **127** 1893–916

García-Serrano J, Cassou C, Douville H, Giannini A and Doblas-Reyes F J 2017 Revisiting the ENSO teleconnection to the Tropical North Atlantic *J. Clim.* **30** 6945–57

Graf H-F and Zanchettin D 2012 Central Pacific El Niño, the "subtropical bridge", and Eurasian climate *J. Geophys. Res.* **117** D01102

Han Z, Luo F and Wan J 2016 The observational influence of the North Atlantic SST tripolar on the early spring atmospheric circulation *Geophys. Res. Lett.* **43** 2998–3003

Hardiman S C, Dunstone N J, Scaife A A, Smith D M, Ineson S, Lim J and Fereday D 2019 The impact of strong El Niño and La Niña events on the North Atlantic *Geophys. Res. Lett.* **46** 2874–83

Hastenrath S, Castro L-C and Aceituno P 1987 The Southern Oscillation in the Atlantic sector *Contrib. Atmos. Phys.* **60** 447–63

Hoskins B J and Ambrizzi T 1993 Rossby wave propagation on a realistic longitudinally varying flow *J. Atmos. Sci.* **50** 1661–71

Hoskins B J and Karoly D J 1981 The steady linear response of a spherical atmosphere to thermal and orographic forcing *J. Atmos. Sci.* **38** 1179–96

Jiménez-Esteve B and Domeisen D I V 2020 Nonlinearity in the tropospheric pathway of ENSO to the North Atlantic *Weather Clim. Dyn.* **1** 225–45

Kidston J, Scaife A A, Hardiman S C, Mitchell D M, Butchart N, Baldwin M P and Gray L J 2015 Stratospheric influence on tropospheric jet streams, storm tracks and surface weather *Nat. Geosci.* **8** 433–40

Klein S A, Soden B J and Lau N-C 1999 Remote sea surface temperature variations during ENSO: evidence for a tropical atmospheric bridge *J. Clim.* **12** 917–32

Lau N-C and Nath M J 2001 Impact of ENSO on SST variability in the North Pacific and North Atlantic: seasonal dependence and role of extratropical air–sea coupling *J. Clim.* **14** 2846–66

Lee S, Enfield D B and Wang C 2008 Why do some el Niños have no impact on tropical north atlantic SST? *Geophys. Res. Lett.* **35** L16705

Li Z X and Conil S 2003 Transient response of an atmospheric GCM to North Atlantic SST anomalies *J. Clim.* **16** 3993–8

Lintner B R and Chiang J C H 2007 Adjustment of the remote tropical climate to El Niño conditions *J. Clim.* **20** 2544–57

Msadek R, Frankignoul C and Li Z X 2011 Mechanisms of the atmospheric response to North Atlantic multidecadal variability: a model study *Clim. Dyn.* **36** 1255–76

Murakami H, Vecchi G A and Delworth T L 2017 Dominant role of subtropical Pacific warming in extreme Eastern Pacific Hurricane seasons: 2015 and the future *J. Clim.* **30** 243–64

Rayner N A *et al* 2003 Global analyses of SST, sea ice and night marine air temperature since the late nineteenth century *J. Geophys. Res.* **108** 4407

Rodwell M J, Rowell D P and Folland C K 1999 Oceanic forcing of the wintertime North Atlantic Oscillation and European climate *Nature* **398** 320–3

Scaife A A *et al* 2017 Predictability of European winter 2015/2016 *Atmos. Sci. Lett.* **18** 38–44

Takaya K and Nakamura H 2001 A formulation of a phase-independent wave-activity flux for stationary and migratory quasigeostrophic eddies on a zonally varying basic flow *J. Atmos. Sci.* **58** 608–27

Taschetto A S, Rodrigues R R, Meehl G A, Mcgregor S and England M H 2016 How sensitive are the Pacific-tropical North Atlantic teleconnections to the position and intensity of El Niño-related warming *Clim. Dyn.* **46** 1841–60

Toniazzo T and Scaife A A 2006 The influence of ENSO on winter North Atlantic climate *Geophys. Res. Lett.* **33** L24704

Wallace J M and Gutzler D S 1981 Teleconnections in the geopotential height field during the northern hemisphere winter *Mon. Weather Rev.* **109** 784–812

Wang C, Kucharski F, Barimalala R and Bracco A 2009 Teleconnections of the tropical Atlantic to the tropical Indian and Pacific Oceans: a review of recent findings *Meteorol. Z* **18** 445–54

Wang Z, Chang C-P, Wang B and Jin F F 2005 Teleconnections from tropics to Northern extratropics through a southerly conveyor *J. Clim.* **62** 4057–70

Webster P J 1981 Mechanisms determining the atmospheric response to sea surface temperature anomalies *J. Atmos. Sci.* **38** 554–71

Webster P J 1982 Seasonality in the local and remote atmospheric response to sea surface temperature anomalies *J. Atmos. Sci.* **39** 41–52

Wen N, Liu Z Y and Li L 2019 Direct ENSO impact on East Asian summer precipitation in the developing summer *Clim. Dyn.* **52** 6799–815

Zhang W, Wang Z, Stuecker M F, Turner A G, Jin F-F and Geng X 2019 Impact of ENSO longitudinal position on teleconnections to the NAO *Clim. Dyn.* **52** 257–74